Available online at www.sciencedirect.com
SCIENCE DIRECT
ELSEVIER
International Journal of Mass Spectrometry 252 (2006) 157–165
International Journal of Mass Spectrometry
www.elsevier.com/locate/ijms

Bulk-like electron–phonon coupling in small free sodium clusters

M. Maier, M. Schätzel, G. Wrigge, M. Astruc Hoffmann, P. Didier, B.V. Issendorff *

Fakultät für Physik, Universität Freiburg, Stefan-Meier-Straße 21, D-79104 Freiburg, Germany

Received 9 November 2005; accepted 21 November 2005
Available online 20 March 2006

Abstract

Free size selected Na_n^+ ($n = 16$–250) clusters have been studied by femtosecond pump-probe photoelectron and photofragmentation spectroscopy. Thermionic electron emission was used to monitor the cooling of the hot electron gas by energy transfer to the ionic background. The results can be well described by the so-called two-temperature model; even for the smallest size no deviation from such bulk-like, continuum model behavior has been observed. Using this theoretical approach we are able to retrieve the electron–phonon coupling constant as a function of the cluster size. In the studied size range the resulting values can be described by the radius dependent function $g(R) = (2.3 + 114\ \text{Å}^2/R^2) \times 10^{16}\ \text{W/m}^3\text{K}$.

PACS: 73.22.−f; 78.47.+p; 79.60.−i

Keywords: Thermionic emission; Photoelectron spectra; Sodium; Weisskopf formalism; Femtosecond experiment; Photofragmentation

1. Introduction

Understanding the physical properties of metallic clusters has become an active field of research because of their importance both for fundamental science [1,2] as well as nanotechnology applications [3,4]. Indeed, finite size effects in such systems confer to them properties that can be very different to those of the bulk. One of the still rather open question is the influence of the finite size on electron relaxation processes like electron–electron and electron–phonon interaction. Especially the latter has been studied in detail for large particles and surfaces. This was mainly done by pump-probe absorption spectroscopy [5–8], but second harmonic generation [9] and electron emission was used as well [10,11]. In all of these studies a similar behavior was found. Absorption of energy from an ultrashort pump laser pulse produces a number of excited electrons; due to the strong electron–electron interaction the energy is redistributed within the electronic system, so that after a short time ($\ll$500 fs) the distribution of excitation energies relaxes into a thermal distribution. This situation can be described as quasi-decoupled partial equilibrium, with a thermalized high temperature electron gas and a low temperature ionic system. The energy transfer between both systems due to electron–phonon coupling takes place on a much longer timescale (with decay times of 1–2 ps). So only after several picoseconds electron gas and ionic system finally are in thermal equilibrium again; the corresponding temperature is in general much lower than the intermediate maximum temperature of the electron gas, because of the much lower heat capacity of the electron system as compared to that of the lattice.

In experiments on metal particles some size dependence was found in the size range from 2 to 100 nm [12,8,5]. This could be explained by the influence of the particle surface, which should get stronger with decreasing particle size. A surface can change the coupling between bulk phonons and electrons due to modified electronic screening [12]; secondly vibrational surface modes exist which exhibit a stronger coupling to electronic excitations [13]. No experiments on medium sized clusters (with a few ten up to a few hundred atoms) have been done yet. Nevertheless this is a very interesting size range, as here a strong influence of the discretized density of states can be expected. Naively termed, simple electron relaxation by single phonon creation gets impossible if the average electron energy level spacing is larger than the Debye frequency, which is the case for simple metal particles with less than about 300 atoms.

We have now studied electron–phonon coupling in exactly this size regime. In order to monitor the time dependent electron gas temperature in these systems we make use of thermal electron emission. This effect, which has been discovered by F.

* Corresponding author.
E-mail address: bernd.von.issendorff@uni-freiburg.de (B.V. Issendorff).

1387-3806/$ – see front matter © 2006 Elsevier B.V. All rights reserved.
doi:10.1016/j.ijms.2005.11.032

Guthrie in 1873, is usually observed for very hot metals, where lattice and electron system are in perfect thermal equilibrium. It has been observed as well in the case of clusters, for example for transition metal clusters [14,15] or C_{60} [16]. It cannot be observed, however, for weakly bound systems like sodium clusters. Such clusters undergo fragmentation at temperatures which are much lower than those necessary for thermal electron emission. Nevertheless thermal electron emission is possible in nonequilibrium situations. As we have recently shown [17,18], by excitation with an ultrashort laser pulse the electron gas in a sodium cluster can easily be heated to several thousand Kelvin, which leads to electron emission rates of several electrons per picosecond. Therefore one or more electrons can be emitted before the electron gas cools down again by electron–phonon energy transfer. The same type of nonequilibrium electron emission from a hot electron gas has been studied in detail for the case of C_{60} [19,20]. As we will show below, this thermal electron emission is very well suited to measure the electron gas cooling rate in a free cluster.

We have studied sodium clusters, as sodium is the best representative of a free electron metal and most easy to treat for theory. So for example for sodium no influence of d-band electrons on the electron–electron and electron–phonon interaction has to be taken into account, in contrast to the case of noble metals [7]. Moreover sodium clusters can be efficiently excited by the standard ultrafast laser photon energy of 3.1 eV, as this energy is close to the strong plasmon resonance of the clusters at about 2.7 eV [21]. So here high excitations can be obtained with relatively weak laser fields ($\leq 10^{10}$ W/cm^2), which means that no strong field effects like field induced tunneling or ionization by recollision events have to be taken into account.

The article is organized as follows: in the first part, we will describe the experimental setup. Then we will present the experimental results and discuss them in the context of a theoretical model; in the last part we will finally summarize and present some perspectives to this work.

2. Experimental techniques

The experimental setup is the same as used in earlier studies [17]. Positively charged sodium clusters of about 200 K temperature are produced in a gas aggregation cluster ion source and mass selected by a double reflectron time-of-flight mass spectrometer. Two types of spectroscopy can be applied to the mass selected clusters: (a) they can be irradiated by a laser pulse in an interaction region before the second reflector, which then serves as a mass analyzer and is used to measure size and charges of the photofragments produced; (b) they can be irradiated in the interaction region of a magnetic bottle type photoelectron spectrometer; in this case the kinetic energy distribution of the emitted electrons is measured.

In order to measure the time evolution of the energy relaxation in the clusters we have used a standard pump-probe setup. Ultrafast pulses delivered by a Ti:sapphire oscillator seed a regenerative and a multipass amplifier, which leads to 120 fs pulses at 800 nm with a repetition rate of 30 Hz. To match the plasmon resonance of sodium clusters, the pulses get converted to 400 nm, 200 fs pulses by second harmonic generation in a 2 mm thick BBO crystal (energy per pulse $\simeq$ 500 μJ). The pulses are split to collinear pump and probe pulses with defined delay time in a Michelson interferometer setup, one arm of which has a variable (and computer controlled) length. A halfwave plate in one of the arms serves to cross-polarize the pulses in order to avoid interference effects for zero delay. In the photoelectron spectrometer the laser beam is collimated by a couple of apertures to a flat top profile with a diameter of 2 mm before it crosses the focused and decelerated ion beam. In the case of photofragmentation measurements the laser beam is collimated by a single aperture to 5 mm diameter. The experimental setup allows us to measure either photoelectron or photofragment distributions as a function of the delay between the pump and the probe laser pulse. The intensity of the laser pulses are usually adjusted to obtain roughly a 50% ionization probability of the irradiated clusters for zero delay time; this requires, depending on the absorption cross sections of the clusters, peak intensities of $1–10 \times 10^9$ W/cm^2.

3. Results and discussion

Pump-probe photoelectron spectra have been measured on Na_n^+ with $n = 16$, 46, 70, 93, 139 and 250. These sizes were chosen in order to both cover a broad size range and to have a selection of electronically closed shell sizes (93 and 139), almost closed shell sizes (46 and 70) and open shell ones (16 and 250). The kinetic energy distributions obtained in the pump-probe experiments were similar to those measured with single pulse excitation, which have been discussed in detail in previous publications [17,18]. In all cases purely exponential energy distributions were obtained. The mean kinetic energy of the electrons exhibits an only weak dependence on the pump-probe delay time; the difference in mean energy between zero delay and large delay times is typically less than 10% under the experimental conditions used. The main pump-probe effect is seen in the total electron intensity. This is demonstrated in Fig. 1, where we present the electron intensity obtained for size selected Na_{16}^+ (Fig. 1a) and Na_{139}^+ (Fig. 1b) as a function of the delay time between the pump and the probe pulse. The two cluster sizes (as well as all other sizes studied) exhibit a similar behavior: maximum electron emission is reached for zero delay between the pump and the probe; with increasing delay the signal decreases, until it reaches a constant value which is approximately twice the intensity produced by the interaction of a single pulse with the cluster. The decrease is symmetrical with respect to zero delay because the pump and the probe are identical except for their polarization direction. In order to get an estimate of the time scales involved, the pump-probe curves have been fitted with a simple exponential decay function:

$$I(\Delta t) = A\left((\beta - 1)\exp\left(-\frac{|\Delta t|}{\tau}\right) + 1\right) \quad (1)$$

Typical values for the decay times of 2 ps were obtained. So what is the physical process responsible for this type of temporal behavior? A statement one can make immediately is that the electron emission we are seeing is not produced by direct mul-

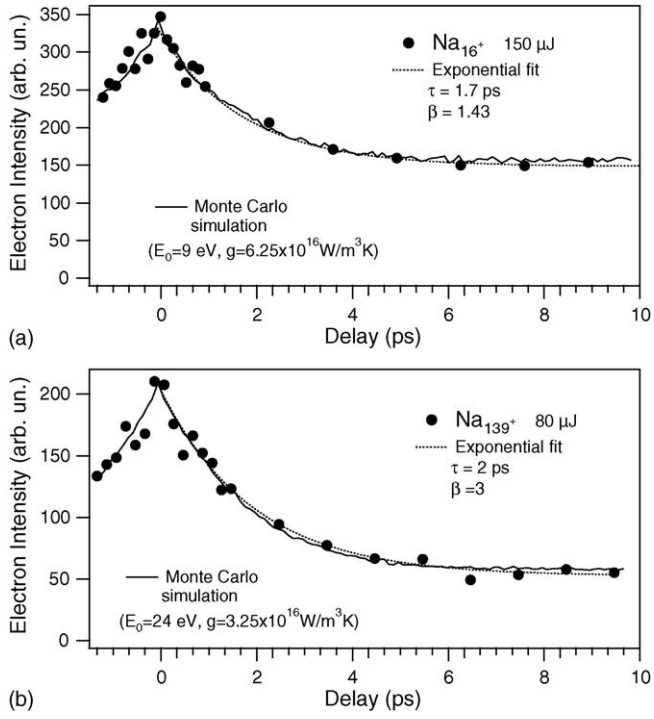

Fig. 1. Photoelectron intensity emitted from Na_{16}^+ (a) and Na_{139}^+ (b) irradiated by 2 fs laser pulses (400 nm, 200 fs) as a function of the delay time between the pulses. The data points have been fitted with simple exponential decay curves (fitting parameters are given) as well as with simulation results as described in the text.

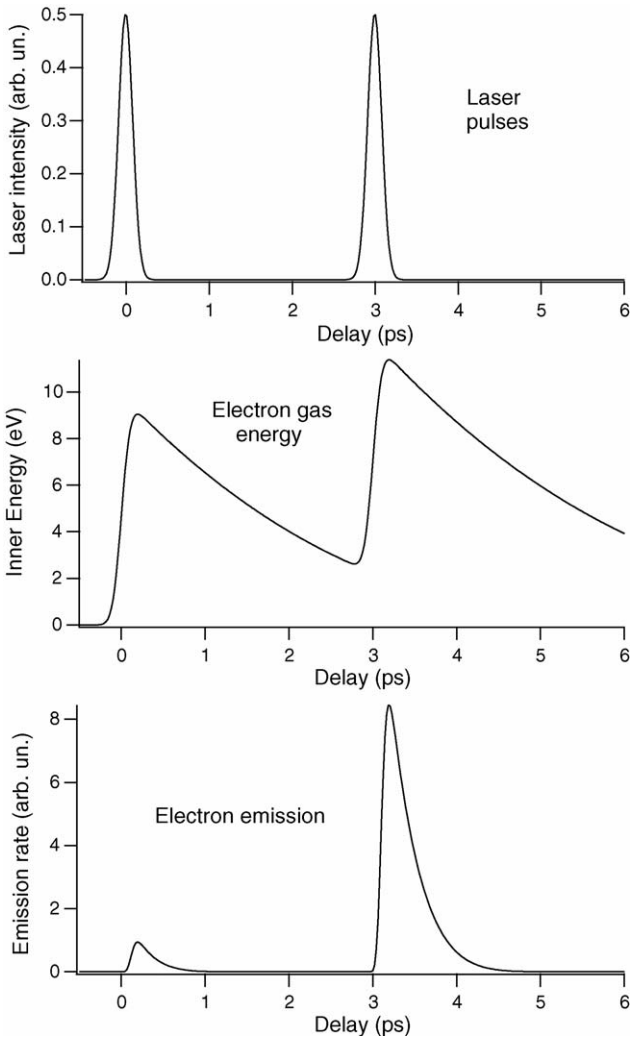

Fig. 2. Schematic of the pump-probe experiment. The electronic system is heated by two laser pulses with variable delay times; delays shorter than the electron gas cooling time lead to enhanced thermal electron emission.

tiphoton ionization of the clusters, which has been discussed as a possible process for sodium clusters in this kind of laser fields [22]. A pump-probe measurement of nonresonant multiphoton ionization should just reflect the field enhancement in the case of pump-probe pulse overlap; the corresponding pump-probe curve should therefore simply be the (second or higher order) autocorrelation curve of the laser pulse, that is a gaussian with a width of less than 200 fs. Multiphoton ionization via intermediate states should reflect the lifetimes of this states. Both the collective plasmon excitation, which is excited at the wavelength used, as well as the single electron excited states produced by the plasmon decay (which therefore have the same energy of ≈3.1 eV), should have lifetimes of less than 100 fs [9,23]. So this cannot explain the observed decay times. Obviously another mechanism plays a role here. As we have discussed previously [17,18], the observed electron intensity and the kinetic energy distributions can be very well explained by thermal electron emission from a hot electron gas, which is only weakly coupled to the vibrational modes of the ionic background. This weak coupling is responsible for the observed temporal behavior as well, as is sketched in Fig. 2. In the pump-probe experiment the cluster is irradiated by two laser pulses of equal intensity, from each of which it absorbs a couple of photons. The intensity of the pulses has been chosen such that the energy absorbed from a single pulse (or from two pulses with a large delay time) leads only to temperatures for which thermal electron emission still is weak. If, however, the second pulse hits the cluster before all of the energy absorbed from the first one has left the electron system, the energy of the electrons will be higher and due to the strongly nonlinear energy dependence of the emission rate (see Fig. 5) one will observe a strongly enhanced electron emission. Measuring the electron intensity as a function of the delay time between the pulses therefore allows one to directly monitor the energy flow out of the electronic system, that is the electron gas cooling by electron–phonon interaction.

If this is true, another effect should be present. As is well known from femtosecond absorption experiments on metallic nanoparticles [6,8], the characteristic time of the electron–phonon thermalization depends on the electronic temperature (that is on the total amount of energy deposited in the system), because of the temperature dependence of the electronic heat capacity. This is indeed the case in our experiment, as one can see in Fig. 3, where we have plotted the normalized electron intensity emitted by Na_{93}^+ clusters for different laser intensities. One can clearly observe different decay times for different degrees of excitation (1.3 and 2.7 ps for 1.6 and 2.9 GW/cm^2 intensity per laser pulse).

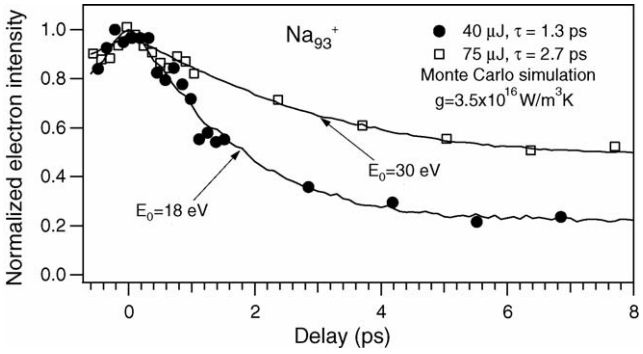

Fig. 3. Pump-probe photoelectron intensity emitted from Na_{93}^+ for two laser intensities. The decay times as obtained from an exponential fit are given; the fitting curves shown are again the result of a full simulation.

In order to check the thermal model quantitatively and to extract the electron–phonon coupling strength from our results, we have simulated the delay curves using the so-called two-temperature model [24]. This model assumes that one can define an electronic and an ionic temperature, which means that the electron and phonon subsystems are each maintained in a thermalized state by electron–electron (coulombic) and phonon–phonon (anharmonic) interaction, while the electron–phonon coupling is weak. The exchange of energy between the hot electron gas and the cold lattice is assumed to be proportional to the temperature difference between the two subsystems. The time dependence of the respective temperatures is hence given by the following two coupled differential equations:

$$c_e(T_e)\dot{T}_e = -g(T_e - T_i) + h\upsilon\sum_n \partial(t - t_n) \tag{2}$$

$$c_i\dot{T}_i = g(T_e - T_i) \tag{3}$$

Here T_e and T_i are the temperatures of the electronic and ionic sub-system, C_e (T) and C_i their respective heat capacities, g is the electron–phonon coupling constant and the last term on the right-hand side in the first equation accounts for the energy increase of the electron gas by photon absorption. For the ions the heat capacity is taken to be the Dulong Petit value ($C_i = 3N_{at}k_B$), whereas the value for the electron gas is calculated from the temperature dependence of the energy of an ideal electron gas:

$$E(T) = \frac{3N_{el}}{2E_F^{3/2}}\int_0^\infty E^{3/2}\left(\exp\left(\frac{E-\mu}{k_BT}+1\right)^{-1}\right)\mathrm{d}E \tag{4}$$

For the Fermi energy the bulk value $E_F = 3.1$ eV is used; the chemical potential μ is determined by the condition that the number of occupied states must be equal to the electron number N_{el}. In order to fully describe the pump-probe signal, one has to take into account the photon statistics. Each photon absorption increases the energy of the electron system. The absorption times t_n are assumed to obey classical statistics; that is the conditional probability for a photon absorption at a time t_n after a preceding event at t_{n-1} is given by:

$$P(t_n|t_{n-1}) = \sigma\Phi(t_n)\exp\left(-\int_{t_{n-1}}^{t_n}\sigma\Phi(t)\mathrm{d}t\right) \tag{5}$$

σ is the cluster absorption cross section and $\Phi(t)$ the laser intensity modeled by two Gaussians with a width of 200 fs ($\tau_L = 85$ fs) and a delay time Δt:

$$\Phi(t) = \frac{\Phi_0}{\tau_L\sqrt{2\pi}}\left[\exp\frac{-(t-t_0)^2}{2\tau_L^2} + \exp\frac{-(t-t_0-\Delta t)^2}{2\tau_L^2}\right] \tag{6}$$

The product of the laser fluence and cluster absorption cross section σ (the total energy absorbed) is used as a fitting parameter, as will be discussed below. In order to describe the thermal electron emission, that is the total electron intensity and the corresponding kinetic energy distributions, we use the statistical theory first proposed by Weisskopf [25]. In this model, the electron emission rate is given by (adopted from [26]):

$$k(E,\varepsilon) = \frac{2m_e\sigma(\varepsilon)}{\pi^2\hbar^3}\varepsilon\frac{\rho(E-\phi-\varepsilon)}{\rho(E)} \tag{7}$$

Here E is the (time dependent) inner energy of the system, ε the kinetic energy of the electrons, m_e the electron mass, and ϕ is the ionization potential. The factor 2 accounts for spin degeneracy. $\sigma(\varepsilon) = \pi r_0^2(1 + (Z+1)e^2/4\pi\varepsilon_0 r_0\varepsilon)$ is the classical capture cross section, where e is the electron charge and Z is the cluster charge before ionization (the image charge is neglected). For the calculation of r_0, the bulk density of sodium was used ($r_0 = \sqrt[3]{N_{at}} \times 2.1$ Å). The multiparticle level density $\rho(E)$ is given by:

$$\rho(E) \propto \exp\left(2\sqrt{\frac{\pi^2}{6}g(E_F)E}\right) \tag{8}$$

with $g(E_F)$ being the free electron gas single particle level density at the Fermi energy:

$$g(E_F) = \frac{3N_{el}}{2E_F} \tag{9}$$

One can now calculate the time-dependent total emission rate for the different charge states simply by integrating over the kinetic energy:

$$K_i(t) = \int_0^{E_i(t)-\phi_i}\frac{2m_e\sigma(\varepsilon)}{\pi^2\hbar^3}\varepsilon\frac{\rho(E_i(t)-\phi_i-\varepsilon)}{\rho(E_i(t))}\,\mathrm{d}\varepsilon \tag{10}$$

Here $E_i(t)$ is the time-dependent internal energy after emission of $(i-1)$ electrons:

$$E_1(t) = E(t)$$
$$E_2(t) = E_1(t) - \phi_1 - \varepsilon_1$$
$$E_3(t) = E_2(t) - \phi_2 - \varepsilon_2$$
$$\vdots$$

where φ_i is the ionization potential of the ith charge state and ε_i the kinetic energy of the ith emitted electron. The ionization potentials are calculated by using:

$$\phi_i = 2.75\,\mathrm{eV} + \frac{(i+0.35)e}{4\pi\varepsilon_0(r_0 + 1\,\text{Å})} \tag{11}$$

which is a fit to previous photoelectron spectroscopy results.

Finally we obtain the following coupled differential equations for the occupation of the different charge states of the cluster which for instance allow us to calculate the total electron intensity as a function of the pump-probe delay:

$$\frac{\mathrm{d}}{\mathrm{d}t}N_1(t) = -N_1(t)K_1(t)$$
$$\frac{\mathrm{d}}{\mathrm{d}t}N_2(t) = N_1(t)K_1(t) - N_2(t)K_2(t)$$
$$\frac{\mathrm{d}}{\mathrm{d}t}N_3(t) = N_2(t)K_2(t) - N_3(t)K_3(t)$$
$$\vdots$$

One parameter which has not been included in this simulation is the spatial laser profile and a possible incomplete overlap of pump and probe laser pulse. To test the importance of this contribution, we have compared the results obtained with a constant (rather flat top profile as in our experiment) and a gaussian profile. The results show that although the total electron intensity does depend on the spatial profile, the delay time dependence is rather insensitive to it. Therefore it was not tried to measure the beam profile in the interaction region and to include this in the calculation.

By Monte Carlo integration of the differential equations (generating photon absorption and electron emission events as well as the electron kinetic energies from random numbers), the number of emitted electrons was calculated as a function of the pump-probe delay time. The electron–phonon coupling constant was varied until the simulated delay curves exhibited the same decay times as the measured ones. The coupling constants obtained in this way have nevertheless a large uncertainty. As has been demonstrated above, the decay times not only depend on the coupling constant, but on the excitation energy as well. It is therefore important to know this excitation energy as precisely as possible. Unfortunately the absorption cross section of the excited cluster is not known, so one cannot use the measured single photon absorption cross section of the cold cluster together with the measured laser fluence to calculate the number of absorbed photons. One possibility to determine the excitation energy is a fit of the measured electron kinetic energy distributions. This is shown in Fig. 4. Here the spectra measured at zero pulse delay time are presented for four different sizes. Using the formalism explained above one can simulate these kinetic energy distributions as a function of the average excitation energy. Examples of best fits (and the parameters used) are included in the graphs. As mentioned already earlier [17], the simulated curves (like the measured ones) are surprisingly perfect exponential curves, although each curve is a superposition of different distributions, because the electrons are emitted from clusters with a broad range of temperatures and charge states.

However, although the measured curves can be fitted quite well with the simulated ones, the uncertainty for the result-

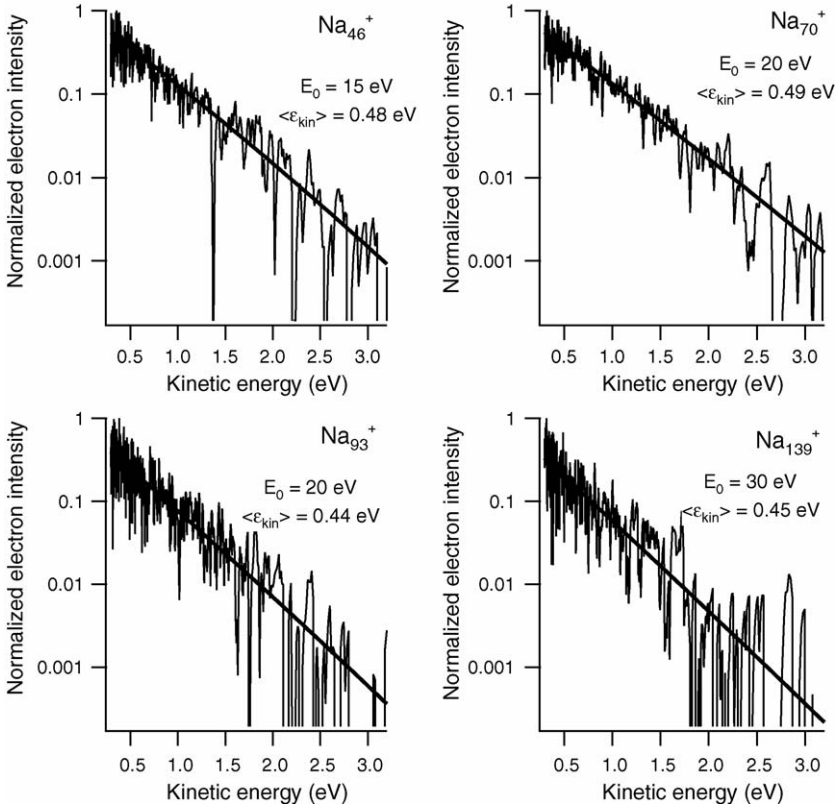

Fig. 4. Kinetic energy distribution of electrons emitted from size selected sodium clusters at zero pump-probe delay time (single 200 fs laser pulse excitation). The spectra have been fitted with simulated kinetic energy distributions (bold solid line). Average excitation energies as used in the simulations are given as well as the mean kinetic energy obtained.

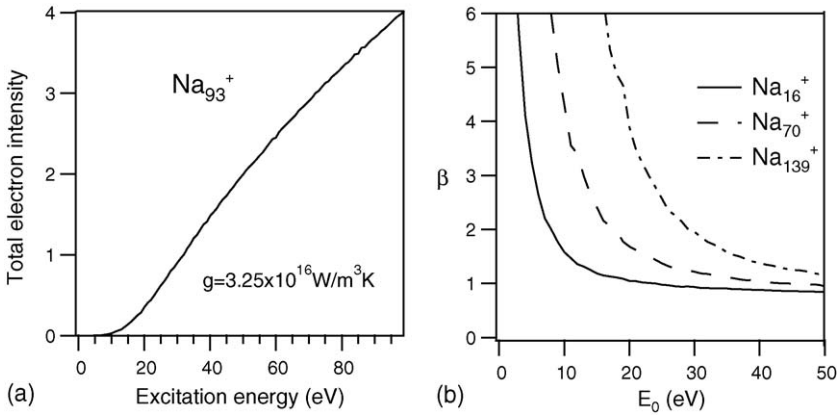

Fig. 5. (a) Simulated total photoelectron intensity as a function of the average energy E_0 absorbed from a single 200 fs pulse for Na_{93}^+. (b) Pump-probe contrast β as a function of E_0 deduced from total electron emission curves as shown in (a), for three different cluster sizes.

ing excitation energy stays rather large, as in fact the average kinetic energy exhibits a rather weak dependence on the degree of excitation [17]. It turns out that the pump probe contrast, the ratio β of electron intensities at zero delay and very large delay times ($\beta = I(0)/I(\infty)$), exhibits a much stronger dependence on the excitation energy than the mean kinetic energies of the electrons. In order to evaluate it we have calculated the electron intensity as a function of the excitation energy for the case of single pulse excitation, again with the methods given above. The result of this calculation for Na_{93}^+ is presented in Fig. 5a. This curve is similar to the one published earlier [17]; it is only somewhat broader, as here the photon absorption statistics have been taken into account, which means that the excitation energy given is the energy absorbed on average. Starting from this curve we are able to estimate the excitation energy dependence of β, which is approximately given by $\beta = I(2E_0)/2I(E_0)$. Fig. 5b presents the variation of β with E_0; from this and the experimental value of β we can deduce the average excitation energy. This approach has been repeated for each cluster size; it yields excitation energies rather close to those obtained from the electron kinetic energy distributions, but with a smaller uncertainty. It actually turns out that the excitation energies obtained from β consistently tend to be 10–15% lower than those obtained from the kinetic energy distributions, which might be due to a slight systematic error of the evaluation of the latter due to the probably oversimplified density of states used (the multiparticle electron density of states has quite an influence on the energy distribution of the electrons, but not so much on the total emission rate – this again makes the pump-probe contrast the preferred value to deduce the excitation energy from).

With this approach we have determined the electron–phonon coupling constants for all sizes studied. The results are presented in Fig. 6.

Although the procedure described above seems to be consistent, one has to keep in mind that the resulting values for the coupling constant are only as good as the determined excitation energies are. Their determination of course strongly relies on the correctness of the Weisskopf model for the description of the electron emission. Even if one does not question the applicability of a statistical model for ultrafast processes in a highly excited small system it is difficult to say how good the two major approximations of the model are. These are using the geometrical cluster cross section as the electron capture cross section and using the multiparticle density of states of a finite electron gas to describe the electron system of the cluster. We have done a couple of tests with modified cross sections and density of states, which turned out not to have a decisive influence; nevertheless an at least partly independent test of the whole model is highly desirable. For this reason we have done a second experiment, a "microcaloric" determination of the electron–phonon coupling constant. As has been demonstrated earlier, one can use the modulation visible in photofragment distributions of sodium clusters to determine their internal energy as well as the number of photons they have absorbed during the excitation [27]. This works not only for singly charged fragments, but for doubly charged ones as well. This is demonstrated in Fig. 7, where mass spectra of doubly charged fragments produced from Na_{93}^+ by irradiation with a 400 nm femtosecond laser pulse are shown. The clusters were thermalized to 220 K before irradiation, due to which they have a very narrow energy distribution. At such a temperature a 93 atom cluster needs to absorb an energy of about 8.5 eV in order to evaporate at least one atom on the time scale of the experiment. More absorbed energy leads to evaporation of more atoms; as the binding energy of one atom is

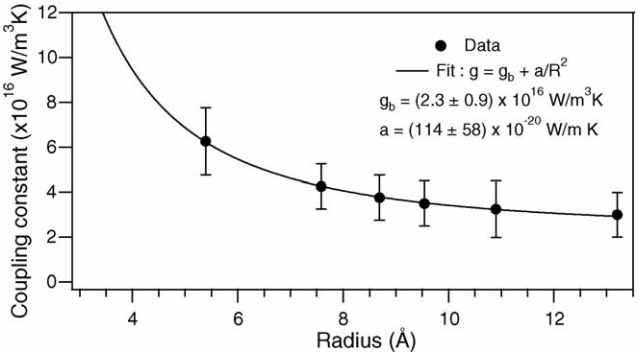

Fig. 6. Electron–phonon coupling constant as a function of the cluster radius (points with error bars). The solid line represents a fit with a tentative fitting function.

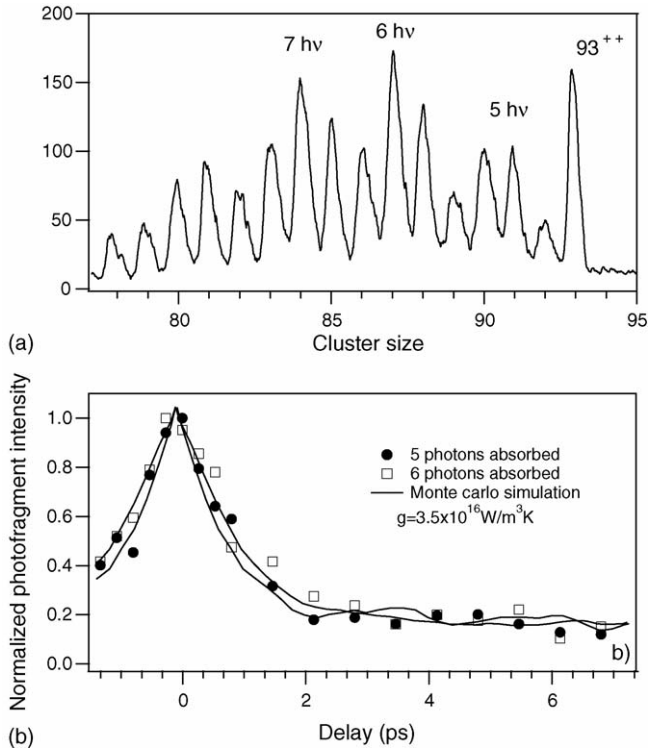

Fig. 7. (a) Mass spectrum of doubly charged photofragments produced from Na_{93}^+ irradiated by a single fs laser pulse (400 nm, 200 fs); (b) Photofragment intensities (of $Na_{90}^{++}/Na_{91}^{++}$ (circles) and $Na_{87}^{++}/Na_{88}^{++}$ (squares)) as a function of the pump-probe pulse delay time.

about 1 eV, for each photon of 3.1 eV about three atoms are emitted. In the case of femtosecond irradiation now the heating of the electron gas can lead to the emission of an electron, which lowers the internal energy of the cluster by the ionization potential (4.6 eV for Na_{93}^+) and the kinetic energy of the emitted electron (here about 0.4 eV on average). The remaining energy is transferred to the lattice and causes the observed atom evaporation. One can therefore identify the first fragment group (sizes $Na_{90}^{++}/Na_{91}^{++}$) as being produced from clusters which have absorbed exactly five photons during the excitation, whereas the second group ($Na_{87}^{++}/Na_{88}^{++}$) results from the absorption of six photons. So the intensities of these doubly charged fragments indicate the electron emission probability after the absorption of a very well defined amount of energy. Measuring these intensities in a pump-probe experiment as a function of the delay time between the laser pulses yields similar curves as the measurements of the total electron intensity. They can be fitted in the same way, with the one important difference that here only one free parameter is used, the electron–phonon coupling constant. In Fig. 7 two pump-probe curves are shown, for five and six photon absorption, respectively. One can see that the decay times are shorter than for the results presented in Figs. 1 and 3; this is due to the fact that in the electron emission measurements the average excitation is stronger (for Na_{93}^+, e.g., the fits give absorbed photon numbers between 7 and 10). Accordingly the six photon curve exhibits a slower decay than the five photon one. Fitting these curves with the model described above (doing a Monte Carlo simulation, but keeping just the results for the specified number of photons absorbed) an electron–phonon coupling constant of 3.5×10^{16} W/m^{3}K is obtained, which is very close to the values obtained from the electron intensity measurements. This agreement gives strong evidence that the modeling used is indeed adequate. One remark should be added with respect to the "microcaloric" measurement technique. In principle it is superior to the measurement of the ensemble averaged photoelectron spectra, but it is applicable only to a limited size range; for too small clusters (less than about 30 atoms) the doubly charged fragments are not stable, but undergo fission. For larger clusters (more than 200 atoms) the atom evaporation statistics broaden the fragment groups to such an extent that single groups cannot be identified anymore. The pump-probe measurement of electron spectra, on the other hand, can be applied to any cluster size, and is therefore more versatile.

We come now back to the results presented in Fig. 6. One can see that the coupling constant decreases with the cluster radius. To our knowledge no rigorous theoretical prediction for the analytical form of the size dependence exists yet. It has been shown that electron-surface–phonon coupling exhibits a predominant $1/R$ and a weaker $1/R^2$ dependence [13] (R being the cluster radius); the correct adding of surface and bulk terms, however, is still under debate [12]. Here we simply rely on the fact that for large sizes the coupling constant must converge to the bulk value, and tentatively use the fitting function:

$$g = g_B + a/R^2 \tag{12}$$

Fitting our results with this formula yield values of $g_B \simeq 2.3 \times 10^{16}$ W/m^{3}K and $a \simeq 110$ Å^2 W/m^{3}K (see Fig. 6). To our knowledge no measurement of the electron–phonon coupling constant for bulk sodium exists which this values could be compared to. Nevertheless an estimate of the constant can be calculated from the electron–phonon spectral function $\alpha^2F(\omega)$ [28]:

$$g_B = \frac{6\hbar}{\pi k_b^2}\gamma \int_0^\infty \alpha^2 F(\omega)\omega \, d\omega \tag{13}$$

The spectral function can be obtained from measured (or calculated) point contact spectra of sodium [29], which gives $\int_0^\infty \alpha^2 F(\omega)\omega \, d\omega = 1.2 \times 10^{25}$ s^{-2}. Using the measured bulk value for the electronic heat capacity ($\gamma = 1.38 \times 10^{-3}$ J/mol K^2) [30], one can then calculate the electron–phonon coupling constant, which gives $g_B = 1.0 \times 10^{16}$ W/m^{3}K. This value is only a factor of two smaller than the one obtained by extrapolation of our results; given all uncertainties of both our data and the "experimental" bulk value this is a rather good agreement. So although the experiments are done on very small systems, and in an extremely high excitation regime (with pump pulse induced intermediate electronic temperatures of up to 7500 K and lattice temperatures of up to 1100 K) an electron lattice energy transfer is observed which is not very different from that of the bulk, and probably converges smoothly to it with increasing size (and decreasing excitation strength). One reason why the smallness of the systems does not lead to dramatically differ-

ent behavior might actually be the high temperatures involved, which can completely mask the discreteness of the density of states. This can be seen by a rough estimate: at an excitation energy of 6.2 eV (absorption of two photons) even the smallest cluster studied, Na_{16}^+, has a multiparticle density of states of $\rho_{tot}(E) \simeq \rho_{tot}(0) \exp\left(\sqrt{\pi^2 N_{el} E/E_F}\right) \simeq 10^7\,eV^{-1}$, which can be considered as a quasi-continuum and certainly allows energy relaxation in steps of the small phonon energies. One should note, however, that this requires the relaxation of multiparticle states. So here electron–phonon coupling has to be seen as the transition from one correlated all electron state to a lower lying, vibrationally more excited one, instead of a single phonon creation connected with the simple transition of one electron from one single particle level to another one, which is the usual model applied in the bulk case. At much lower excitation energies the discreteness even of the multiparticle density of states should nevertheless influence the electron–phonon interaction. This will be studied in future experiments.

Finally we would like to come back to the issue of direct electron emission, that is electron emission via a multiply excited plasmon, as postulated in [31] and treated by several theoretical studies [32,22,33]. Such a direct emission should have a different energy distribution (nonthermal in any case [22], but possibly structured as well [34,33]), and a different temporal behavior (strongly peaked pump-probe curve due to the very short lifetime of the plasmon). No such effect was observed. This does not mean, however, that direct electron emission does not take place; in our experiment it is probably not visible only because of the very strong intensity of thermal electrons. In order to observe the direct processes, one has to use much shorter laser pulses, which have a peak intensity sufficient for multiple plasmon excitation, but a total energy smaller than what is necessary to cause a strong heating of the electron gas. For Na_{93}^+, e.g., at least five photons have to be a absorbed to cause appreciable thermal electron emission. On the other hand, one would like to have a good probability for the absorption of two photons within the lifetime of the plasmon ($\leq$10 fs). It follows that one should use laser pulses of less than about 30 fs width, with an intensity that lead to the absorption of about three to four photons from one pulse. Additionally it is possible to distinguish direct from thermal electrons by measuring their angular distribution. Thermal electrons should be emitted perfectly isotropically [15], whereas direct electrons are predicted to have strongly peaked angular distributions [22,33]. Therefore currently an experiment is being set up which will allow the measurement of the angular distributions of photoelectrons emitted from clusters under $\approx$30 fs laser pulse irradiation.

4. Conclusion

By using femtosecond pump-probe photoelectron and photofragmentation spectroscopy, we have investigated the thermal electron emission of size-selected Na_n^+ clusters (n = 16–250). We have measured the time-dependent electron intensity and kinetic energy distribution for all of these clusters as well as the time-dependent intensity of doubly charged photofragments for Na_{93}^+. The results can be described in the framework of the two-temperature model, coupled to the statistical formalism of Weisskopf, which allowed us to deduce the electron–phonon coupling constants of the clusters. The values obtained are on the order of 4×10^{16} W/m^{3}K and decrease with increasing cluster radius.

Extrapolation of the results yields an estimate for the bulk electron–phonon coupling constant of sodium: $g_B \simeq 2.3 \pm 1 \times 10^{16}$ W/m^{3}K.

Acknowledgement

This work was supported by the Deutsche Forschungsgemeinschaft.

References

[1] W. de Heer, Rev. Mod. Phys. 65 (1993) 611.
[2] H. Haberland (Ed.), Clusters of Atoms and Molecules I&II, Springer-Verlag, Berlin, 1994.
[3] L. Cognet, C. Tardin, D. Boyer, D. Choquet, P. Tamarat, B. Lounis, PNAS 100 (2003) 11350.
[4] G. Reiss, A. Hütter, Nat. Mater. 4 (2005) 725.
[5] M. Nisoli, S. Stagiara, S. De Silvestri, A. Stella, P. Tognini, P. Cheyssac, R. Kofman, Phys. Rev. Lett. 78 (1997) 3575.
[6] S. Link, M.A. El-Sayed, J. Phys. Chem. B 103 (1999) 8410.
[7] A. Arbouet, C. Voisin, D. Christofilos, P. Langot, N. Del Fatti, F. Valleé, J. Lermé, G. Celep, E. Cottancin, M. Gaudry, M. Pellarin, M. Broyer, M. Maillard, M.P. Pileni, M. Treguer, Phys. Rev. Lett. 90 (2003) 7401.
[8] G.V. Hartland, Phys. Chem. Chem. Phys. 6 (2004) 5263.
[9] J.-H. Klein-Wiele, P. Simon, H.-G. Rubahn, Phys. Rev. Lett. 80 (1998) 45.
[10] M. Merschdorf, W. Pfeiffer, S. Voll, G. Gerber, Phys. Rev. B 68 (2003) 155416.
[11] J.G. Fujimoto, J.M. Liu, E.P. Ippen, N. Bloembergen, Phys. Rev. Lett. 53 (1984) 1837.
[12] J. Lermé, G. Celep, M. Broyer, E. Cottancin, M. Pellarin, A. Arbouet, D. Christofilos, C. Guillon, P. Langot, N. Del Fatti, F. Valleé, Eur. Phys. J. 34 (2005) 199.
[13] E.D. Belotskii, P.M. Tomchuk, Int. J. Electron. 73 (1992) 955.
[14] G. Ganteför, W. Eberhardt, H. Weidele, D. Kreisle, E. Recknagel, Phys. Rev. Lett. 77 (1996) 4524.
[15] J.C. Pinare, B. Baguenard, C. Bordas, M. Broyer, Phys. Rev. Lett. 81 (1998) 2225.
[16] E.E.B. Campbell, G. Ulmer, I.V. Hertel, Phys. Rev. Lett. 97 (1991) 1986.
[17] R. Schlipper, R. Kusche, B.V. Issendorff, H. Haberland, Appl. Phys. A 72 (2001) 255.
[18] M. Maier, M. Astruc Hoffmann, B.V. Issendorff, NJP 5 (2003) 3.1.
[19] E.E.B. Campbell, K. Hansen, K. Hoffmann, G. Korn, M. Tchaplyguine, M. Wittmann, I.V. Hertel, Phys. Rev. Lett. 84 (2000) 2128.
[20] K. Hansen, K. Hoffmann, E.E.B. Campbell, J. Chem. Phys. 119 (2003) 2513.
[21] T. Reiners, C. Ellert, M. Schmidt, H. Haberland, Phys. Rev. Lett. 74 (1995) 1558.
[22] A. Pohl, P.-G. Reinhard, E. Suraud, J. Phys. B: At. Mol. Opt. Phys. 37 (2004) 3301.
[23] M. Bauer, M. Aeschlimann, J. Elect. Spect. Rel. Phen. 124 (2002) 225.
[24] S.I. Anisimov, B.L. Kapeliovich, T.L. Perel'man, Sov. Phys. JETP 39 (1974) 375.
[25] V. Weisskopf, Phys. Rev. 52 (1937) 295.
[26] J.M. Weber, K. Hansen, M.-W. Ruf, H. Hotop, Chem. Phys. 239 (1998) 271.

[27] M. Schmidt, R. Kusche, W. Kronmüller, B.V. Issendorff, H. Haberland, Phy. Rev. Lett. 79 (1997) 99.
[28] P.B. Allen, Phys. Rev. Lett. 59 (1987) 1460.
[29] R. Bauer, A. Schmid, P. Pavone, D. Strauch, Phys. Rev. B 57 (1998) 11276.
[30] C. Kittel, Introduction to Solid State Physics, John Wiley and Sons, New York, 1996.
[31] R. Schlipper, R. Kusche, B.V. Issendorff, H. Haberland, Phys. Rev. Lett. 80 (1998) 1194.
[32] G.F. Bertsch, N. Van Giai, N. Vinh Mau, Phys. Rev. A 61 (2000) 033202.
[33] L.G. Gerchikov, A.N. Ipatov, J. Phys. B: At. Mol. Opt. Phys. 36 (2003) 1193.
[34] A. Pohl, P.-G. Reinhard, E. Suraud, Phys. Rev. Lett. 84 (2000) 5090.